International Journal of Power Electronics and Drive System (IJPEDS)
Vol. 8, No. 4, December 2017, pp. 1682~1692
ISSN: 2088-8694, DOI: 10.11591/ijpeds.v8i4.pp1682-1692

Comparison Performances of Indirect Field Oriented Control for Three-Phase Induction Motor Drives

Hasif Aziri[1], Fizatul Aini Patakor[2], Marizan Sulaiman[3], Zulhisyam Salleh[4]
[1,3]Faculty of Electrical Engineering, Universiti Teknikal Malaysia Melaka, Malaysia
[2]Department of Electrical Engineering, Politeknik Merlimau Melaka, Malaysia
[4]Department of Electrical Engineering, Politeknik Melaka, Malaysia

Article Info

Article history:

Received Sep 6, 2017
Revised Oct 10, 2017
Accepted Oct 30, 2017

Keyword:

Field oriented control
Induction motor
PI controller
PSIM
Speed controller

ABSTRACT

This paper presents the comparative performances of Indirect Field Oriented Control (IFOC) for the three-phase induction motor. Recently, the interest of widely used the induction motor at industries because of reliability, ruggedness and almost free in maintenance. Thus, the IFOC scheme is employed to control the speed of induction motor. Therefore, P and PI controllers based on IFOC approach are analyzed at differences speed commands with no load condition. On the other hand, the PI controller is tuned based on Ziegler-Nichols method by using PSIM software which is user-friendly for simulations, design and analysis of motor drive, control loop and the power converter in power electronics studies. Subsequently, the simulated of P controller results are compared with the simulated of PI controller results at difference speed commands with no load condition. Finally, the simulated results of speed controllers are compared with the experimental results in order to explore the performances of speed responses by using IFOC scheme for three-phase induction motor drives.

Copyright © 2017 Institute of Advanced Engineering and Science.
All rights reserved.

Corresponding Author:

Hasif Aziri,
Department of Electrical Engineering,
Universiti Teknikal Malaysia Melaka,
Hang Tuah Jaya, 76100 Durian Tunggal,
Melaka, Malaysia.
Email: hasifaziri@gmail.com

1. INTRODUCTION

Recently, the three phase induction motors are generally employed for control and automation industries. The interest of widely used the induction motor at industry because of reliability, ruggedness and almost free in maintenance [1]. However, the working condition of induction motors are based on parameters which deteriorates the reliability and decrease the performance due to the nonlinearity and complexity of motor model [2]. Therefore, various methods are proposed in [3]-[5] which are good to maintain the motor performances, but not practical for applications because of complicated issues for implementation.

In fact, the classical control techniques are based on Field-Oriented Control (FOC) scheme is employed with the simplest regulator such as the proportional (P), proportional-integral (PI) and proportional-integral-derivative (PID) controllers. In addition, the PI and PID controllers are commonly used to regulate torque, current and speed because of the simplicity for implementation [6]. However, these controllers are sensitive to motor parameters and load variations. Furthermore, the control structure of these controllers also despite a comprehensive tuning based on parameters such as proportional, K_p, integral, K_i and derivative, K_d. Hence, the set of tunings will end up with different parameters. Therefore, the approach of speed controller tuning is plenty of motivation to develop an algorithm. In advanced control techniques, the most common control algorithm for speed regulators are based on Fuzzy Logic Controller (FLC), Sliding

Mode Controller (SMC) and Artificial Neural Network (ANN) whether by using an intelligent or an adaptive control algorithm. Accordingly, the FLC are provides a good dynamic performances and robustness to parameters variations, while SMC are excellent for system order rejection, disturbance rejection and easy for implementation [7]. Besides, the ANN are able to accommodate the complicated of arbitrary and nonlinearity [8]. However, these controllers approach has its own disadvantages and advantages due to the several factors such as the robustness towards parameter changes and external disturbances, the response time, the computing time, simplicity to the design and implementation.

Specifically, the comparison performances of IFOC for three-phase induction motor drives are established in this paper. Accordingly, the section 2 defines the modelling of induction motor while, the section 3 describes the indirect field-oriented control scheme. Then, the section 4 demonstrated about simulation and hardware setup while, section 5 devoted about simulated and experimental results. Finally, the conclusion, acknowledgments and references are listed at the end of this paper.

2. MODELING OF INDUCTION MOTOR

The linearity of stator and rotor with three-phase balance and symmetrical structure are assumed by dynamic modeling derivations of induction motor. Specifically, the both reference frame of stator and rotor are customarily derived in synchronously from equations of motion, voltage and flux linkage [9]. The dq-axis of equivalent model for induction motor is achieved by decoupling an imaginary part and real part from space vector model with equations of motion, voltage and flux linkage respectively as shown in Figure 1.

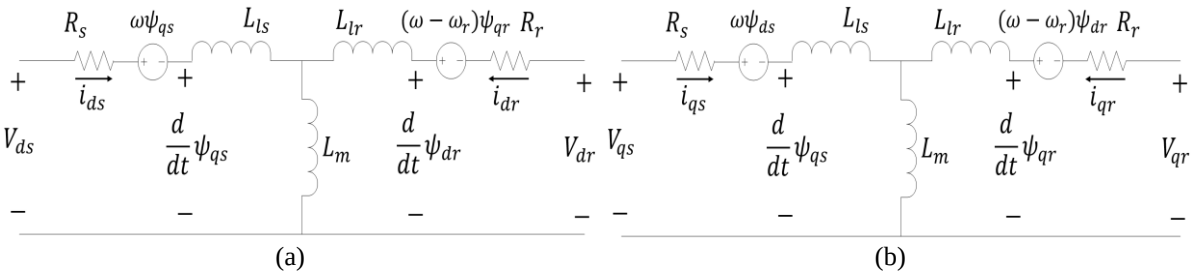

Figure 1. The dq-axis of equivalent model; a) d-axis b) q-axis for induction motor

The voltage equations for both reference frame of stator and rotor in dq-axis that corresponding to the flux linkages are described as:

$$V_{ds} = R_s I_{ds} + \frac{d\psi_{ds}}{dt} - \omega\psi_{qs} \quad (1)$$

$$V_{qs} = R_s I_{qs} + \frac{d\psi_{qs}}{dt} + \omega\psi_{ds} \quad (2)$$

$$V_{dr} = R_r I_{dr} + \frac{d\psi_{dr}}{dt} - (\omega - \omega_r)\psi_{qr} \quad (3)$$

$$V_{qr} = R_r I_{qr} + \frac{d\psi_{qr}}{dt} + (\omega - \omega_r)\psi_{dr} \quad (4)$$

Where V_{ds}, V_{qs} and V_{dr}, V_{qr} are defined as the stator of dq-axis voltage and the rotor of dq-axis voltage. The stator and rotor resistances are defined by R_s and R_r while, I_{dr}, I_{qr} and I_{ds}, I_{qs} are demonstrated as the dq-axis of rotor current and the dq-axis of stator current. Then, ψ_{dr}, ψ_{qr} and ψ_{ds}, ψ_{qs} are demonstrated as the dq-axis rotor of flux linkage and the dq-axis stator of flux linkage. Hence, ω_r and ω are represented as rotation of electrical speed and arbitrary reference frame of speed rotation, respectively.

The flux linkage of dq-axis in terms of equivalent equations are specified as:

$$\psi_{ds} = L_s i_{ds} + L_m i_{dr} \quad (5)$$

$$\psi_{qs} = L_s i_{qs} + L_m i_{qr} \quad (6)$$

$$\psi_{dr} = L_r i_{dr} + L_m i_{ds} \quad (7)$$

$$\psi_{qr} = L_r i_{qr} + L_m i_{qs} \quad (8)$$

Where L_r and L_s are defined as self-inductance of rotor and stator while, L_{lr} and L_{ls} are represented as leakage inductance of rotor and stator. Then, L_m is demonstrated as magnetizing inductance that measured in Henry(H) while, $L_r = L_{lr} + L_m$ and $L_s = L_{ls} + L_m$, respectively.

The stator and rotor of dq-axis model are substituting from Eq. (5)-(8) into Eq. (1)-(4) are stated as:

$$V_{ds} = R_s I_{ds} - \omega\psi_{qs} + L_{ls}\frac{d}{dt} I_{ds} + L_m \frac{d}{dt}(I_{ds} + I_{dr}) \quad (9)$$

$$V_{qs} = R_s I_{qs} + \omega\psi_{ds} + L_{ls}\frac{d}{dt} I_{qs} + L_m \frac{d}{dt}(I_{qs} + I_{qr}) \quad (10)$$

$$V_{dr} = R_r I_{dr} - (\omega - \omega_r)\psi_{qr} + L_{lr}\frac{d}{dt} I_{dr} + L_m \frac{d}{dt}(I_{ds} + I_{dr}) \quad (11)$$

$$V_{qr} = R_r I_{qr} + (\omega - \omega_r)\psi_{dr} + L_{lr}\frac{d}{dt} I_{qr} + L_m \frac{d}{dt}(I_{qs} + I_{qr}) \quad (12)$$

Where the above Eq. (9) – (12) is depicted in Figure 1 for the dq-axis equivalent model which are Figure 1(a) is d-axis equivalent model and Figure 1(b) is q-axis equivalent model.

The motion equation from space vector model is manipulated in various approach to demonstrated the equation of electromagnetic torque, T_e. Hence, the frequently used equations are expressed either combine dq-stator current with rotor and stator of flux linkage equation or expressed as dq-stator with rotor current as presented below:

$$T_e = \begin{cases} \frac{3P}{2}(i_{qs}\psi_{ds} - i_{ds}\psi_{qs}) \\ \frac{3PL_m}{2}(i_{qs}i_{dr} - i_{ds}\psi_{qr}) \\ \frac{3PL_m}{2L_r}(i_{qs}\psi_{dr} - i_{ds}\psi_{qr}) \end{cases} \quad (13)$$

Correspondingly, the ultimate equations of motion and electromagnetic torque to perform for simulation are defined as:

$$\frac{d\omega_m}{dx} = \frac{P}{J}(T_e - T_m) \quad (14)$$

$$T_e = \frac{3P}{2}(i_{qs}\psi_{ds} - i_{ds}\psi_{qs}) \quad (15)$$

Where ω_m is stated as the mechanical rotor speed (rad/s) while, the inertia (kgm^2) is represented by *J* and the number of poles is represented by *P*. Then, T_m is stated as the mechanical torque ($N.m$) while, T_e is represented as electromagnetic torque.

3. INDIRECT FIELD-ORIENTED CONTROL SCHEME

The IFOC scheme is obtained into direct control and indirect control schemes based on classifications of field angle. In particular, the direct field-oriented control scheme is recognized when the

acquired field angle is used by windings of flux sensing or terminal currents and voltages. Besides, the indirect field-oriented control scheme is recognized when the calculated field angle is not used voltage or current as variables from the rotor position [10]. On the other hand, the principal approach of IFOC is to controlling separately excited with the DC motor by independently control the torque and flux in the induction motor [11]. Therefore, IFOC is commonly used by researchers in order to develop or improve the performance of induction motor drive. Other than that, the fundamental principal of IFOC is demonstrated in phasor diagram as shown in Figure 2 [12].

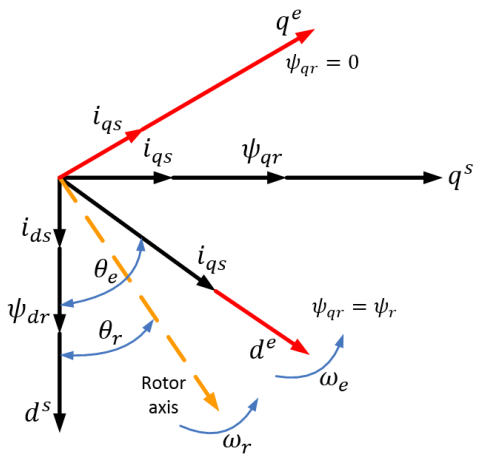

Figure 2. The phasor diagram of IFOC scheme

In Figure 2, the stator is settled by the $d^s - q^s$, the rotor is settled by the $d^r - q^r$ and the synchronous rotor is settled by $d^e - q^e$. Moreover, the references frame from the q-axis of rotor field is assumed to be zero ($\psi_{qr} = 0$) and the rotor current equation is obtained as:

$$\psi_{qr} = L_r i_{qr} + L_m i_{qs} = 0, \qquad I_{qr} = \frac{-L_m}{L_r} i_{qs} \tag{16}$$

Basically, the q-axis of stator current and slip of angular frequency can be calculated to control the electromagnetic torque. Further, the d-axis of stator current can be used to calculated the d-axis of rotor flux as presented in the following equations.

$$\psi_{dr} = \frac{R_r L_m}{R_r + \frac{dL_r}{dt}} i_{ds} \tag{17}$$

$$\psi_{dr} = \frac{R_r L_m}{R_r + \frac{dL_r}{dt}} i_{ds} \tag{18}$$

$$\omega_{sl} = \omega_e - \omega_r = \int (\theta_e - \theta_r) dt = \frac{R_r i_{qs}}{L_r i_{ds}} \tag{19}$$

Where the electrical and rotor of angular frequencies are represented by ω_e, ω_r while, the synchronous and rotor of angle speed are represented by θ_e, θ_r. Then, ω_{sl} is define as the slip of angular frequency.

4. SIMULATION AND HARDWARE SETUP

The setup of simulation is performed by using PSIM software. Specifically, this software provides a powerful simulation environment for motor control and power electronics studies. Moreover, the design and analysis of motor drive, control loop and power converter are also supported with PSIM software. The process of simulation setup is illustrated in Figure 3. On the other hand, the schematic of three-phase induction motor drives by using IFOC is depicted in Figure 4 and Figure 5.

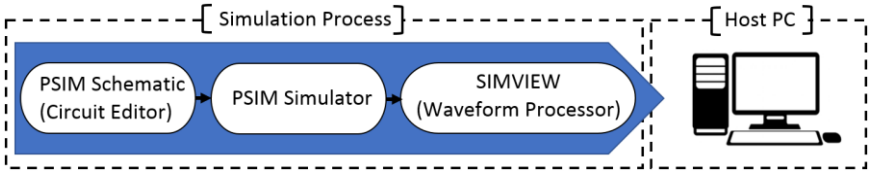

Figure 3. The process of simulation setup by using PSIM software

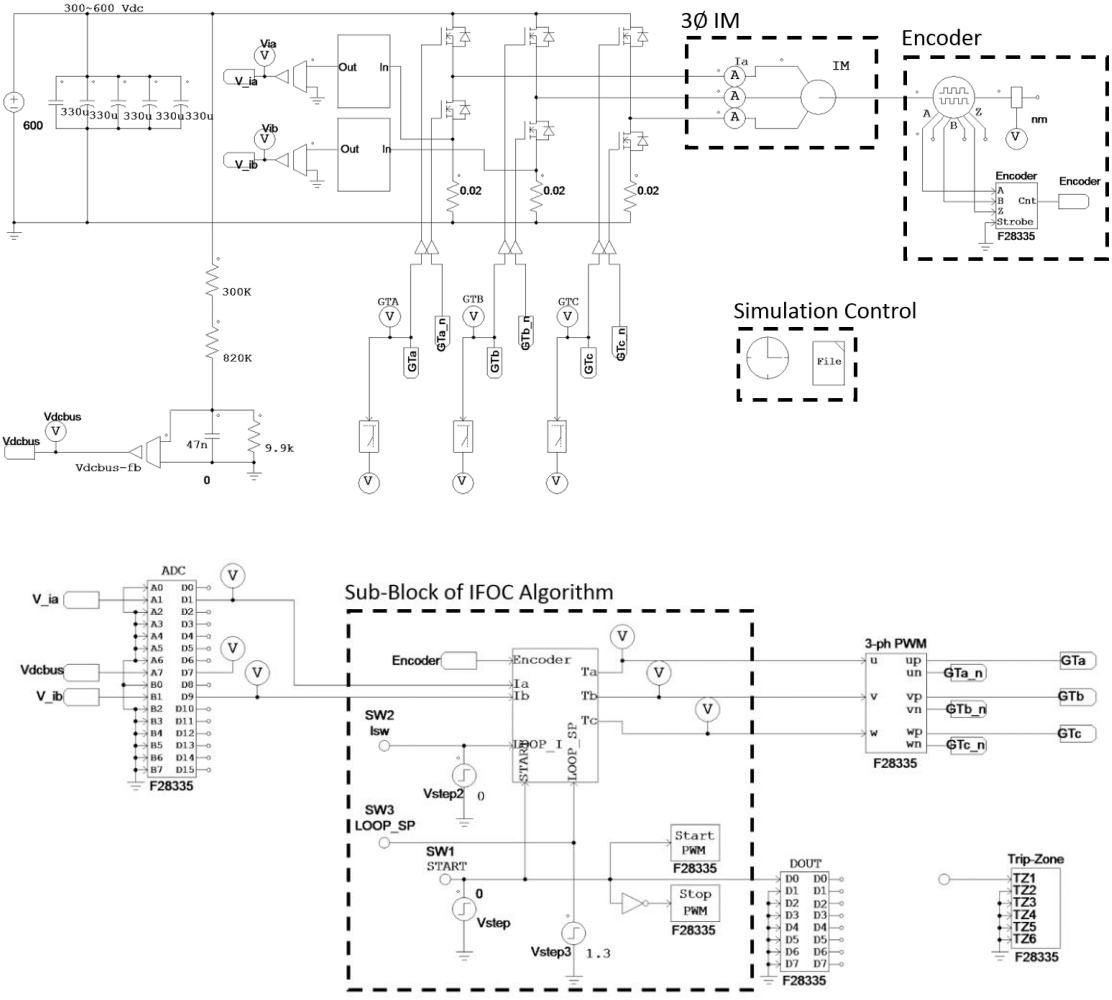

Figure 4. The schematic of three-phase induction motor drives based on TMS320F28335 DSP

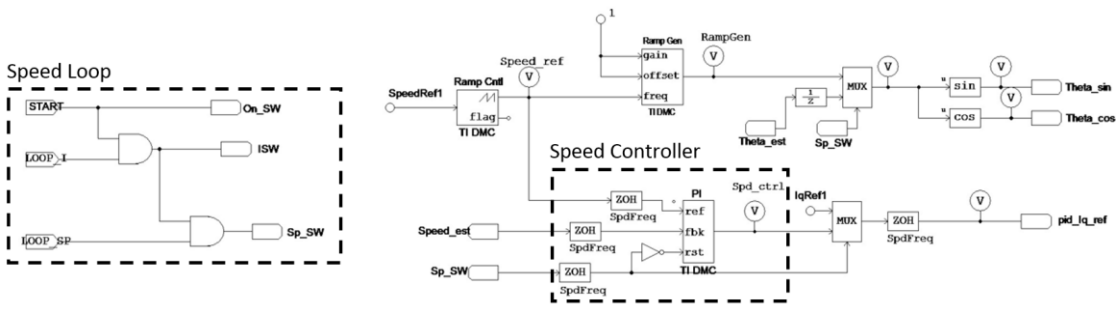

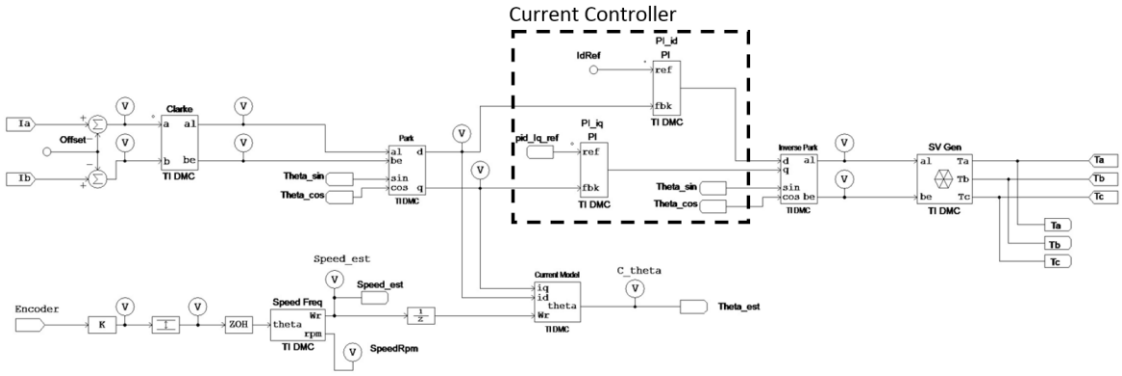

Figure 5. The sub-block of IFOC algorithm for three-phase induction motor drives

The setup of hardware for experimental work is based on High Voltage Digital Motor Control (DMC) with Power Factor Correction (PFC) from Texas Instruments. The DMC with PFC board is capable for sensored and sensorless Field Oriented Control (FOC) of high voltage PMSM, BLDC and AC induction motors. The DMC also can cover DC maximum input voltage is up to 350V with 1kW maximum load while, PFC stage rated is 750W with maximum output voltage is up to 400V that rectified from AC input of 110V AC or 220V AC [13]. Noted that the experiment is based on the TMS320F28335 DSP and used the three-phase induction motor with rated at 220V AC. Moreover, the variable AC transformer is used when starting the experiment for a safety purpose. Hence, the PC desktop act as a host to monitor setting, giving commands and evaluating results from the DMC C2000 system user interface. Hence, the rotor speed of induction motor is monitored by using encoder that attached on the induction motor shaft which is connected to the DMC board platform. Specifically, the hardware setup for the drive system is demonstrated in Figure 6 and the overall block diagram of IFOC for three-phase induction motor drive is depicted in Figure 7.

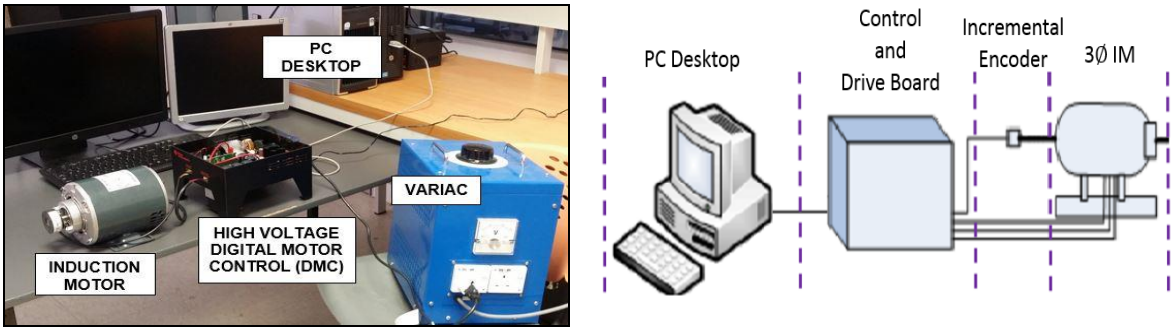

(a) (b)

Figure 6. The setup for drive system; (a) experimental test, (b) hardware configuration

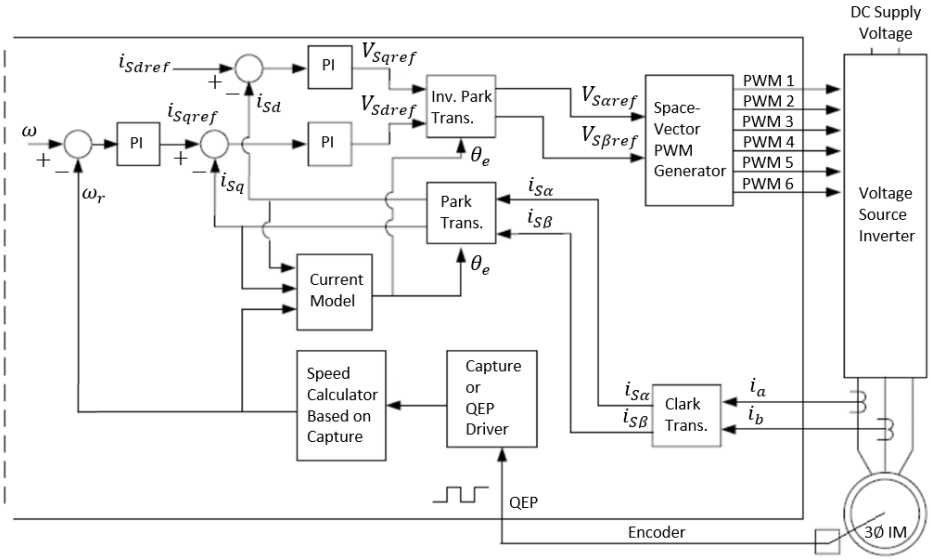

Figure 7. The overall block diagram of IFOC for three-phase induction motor drives

5. SIMULATION AND HARDWARE SETUP

The overall system for simulation and experimental are implemented with three-phase symmetrical squirrel-cage induction motor. In addition, the rated speed of induction motor is 1725rpm with 60Hz base electrical frequency. Hence, the base peak current voltage value is 376V while, the base peak current value is 3A respectively. Other than that, the motor parameters of three-phase induction motor are shown in Table 1. Furthermore, the simulation and experimental cases are observed in term of speed commands with no load condition as shown in Table 2.

Table 1. Induction Motor Parameters

Parameters	Specifications
Rs (stator)	11.05 Ω
Ls (stator)	6.11 H
Rr (rotor)	0.32 Ω
Lr (rotor)	0.32 H
Lm (magnetizing)	0.29 H
No. of Pole	4
Moment of Inertia	0.91 kg.m^2

Table 2. Simulation and Experimental Cases

Cases	Speed Commands (rpm)
1	Full rated speed = 1500
2	Half rated speed = 900
3	Low rated speed = 450

Initially, the simulated results are tuning based on Ziegler-Nichols method which is commonly used to tuning of PI and PID control algorithm. The tuning method was the first published by Ziegler and Nichols in 1942. In particular, the controller coefficients are tuning based on parameters such as proportional, integral and derivative [14]. On the other hand, the set of tunings will end up with different parameters. So, the approach of speed controller tuning is plenty of motivation to develop an algorithm [15]. The tuning based on Ziegler-Nichols method consist of the following steps:

1. Reduce the integrator, $\tau_I = K_i$ and derivative, $\tau_D = K_d$ gains to 0 values. Noted that, the value controller gain is called, K_{cu} and the peak to peak period is called, P_u.

2. Increase $K_c = K_p$ from 0 to continuous oscillation that also called as critical or ultimate gain, K_{cu}. Noted that, the slightly larger value of controller gain will be giving unstable closed loop system while for slightly lower value will stable the system but giving a slow response.
3. The tuning parameters are referring on the Table 3 base on the critical gain and period of chosen P, PI, or PID controllers. Noted that, the rules of tuning parameters that result in less sensitivity and oscillatory responses in the process condition are suggested by Tyrees and Luyben as shown in Table 4 [16].

Table 3. Ziegler-Nichols Method Tuning Parameters

Controller Type	K_c	τ_I	τ_D
P	$0.5K_{cu}$	∞	-
PI	$0.45 K_{cu}$	$P_u/1.2$	-
PID	$0.6K_{cu}$	$P_u/2$	$P_u/8$

Table 4. Tyrees-Luyben Suggested Tuning Parameters Based on Ziegler-Nichols Tuning Method

Controller Type	K_c	τ_I	τ_D
PI	$K_{cu}/3.2$	$2.2P_u$	-
PID	$K_{cu}/2.2$	$2.2P_u$	$P_u/6.3$

Figure 8 shows the simulated results of P and PI controllers at differences speed commands with no load condition. In particular, the tuning parameters for P controller are $K_p = 1$ and $K_i = 0$ while, for PI controller are $K_p = 1$ and $K_i = 0.2$ respectively. Then, Figure 7 (a) shows the P control is contributed less overshoot and PI control is almost zero overshoot but slower than P and PI controllers in Figure 8 (b) and Figure 8 (c) to achieve steady step response at full rated speed condition. Besides, Figure 8 (b) shows the P and PI controllers are contributed less overshoot and faster than P and PI controllers in Figure 8 (a) but slower than P and PI controllers in Figure 8 (c) at half rated speed. Hence, Figure 8 (c) shows the P and PI controllers are produced chattering and oscillatory responses but contributes shorter time than P and PI controllers in Figure 8 (a) and Figure 8 (b) to achieve steady step response at low rated speed condition. Therefore, the comparison of P and PI controllers are noted that the PI controller is more outstanding than the P controller at differences speed commands with no load condition.

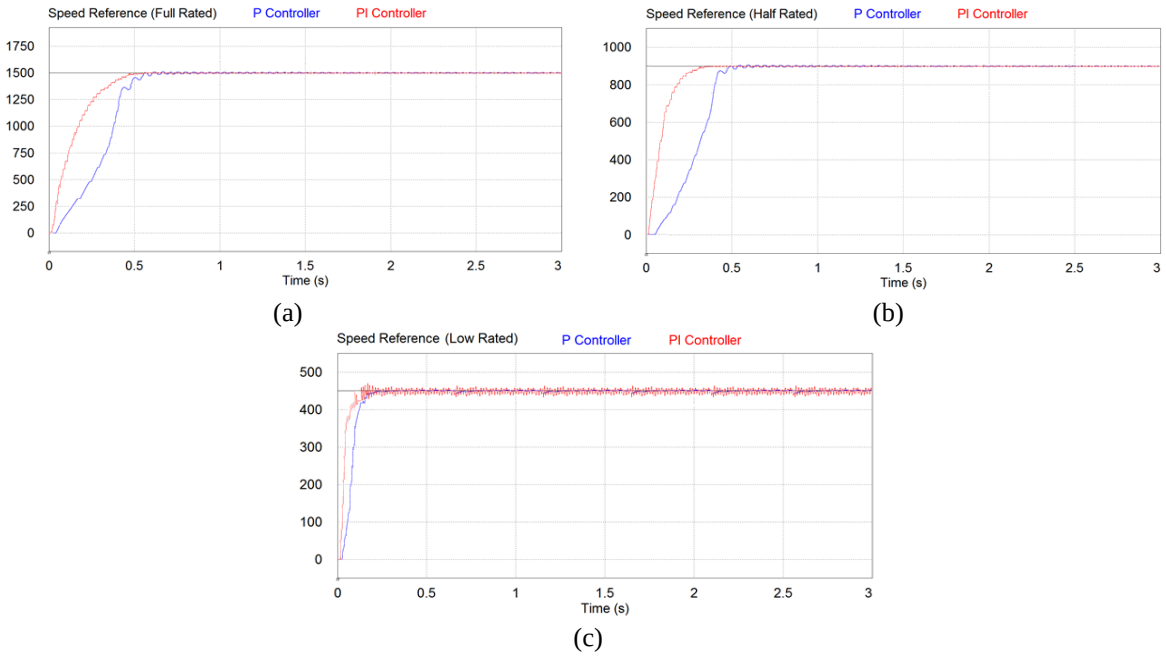

Figure 8. Simulated of P and PI results at; (a) full, (b) half and (c) low rated

Figure 9 shows the simulated and experimental of PI speed controller results at difference speed commands with no load condition. In further, the tuning parameters for PI controller are $K_p = 1$ and $K_i = 0.2$ respectively. Besides, Figure 9 (a) shows the simulated result and Figure 9 (b) shows the experimental result is contributed almost zero overshoot but slower than the simulated and experimental results in Figure 9 (c)-(f) to achieve steady step response at full rated speed condition. Then, Figure 9 (c) shows the simulated result and Figure 9 (d) shows the experimental result is contributed less overshoot and oscillatory responses but slower than simulated and experimental results in Figure 9 (e)-(f) and faster than simulated and experimental results in Figure 9 (a)-(b) to achieve steady step response at half rated speed condition. Hence, Figure 9 (e) shows the simulated result and Figure 9 (f) shows the experimental result is produced chattering and oscillatory responses but contributes faster time than simulated and experimental results in Figure 9 (a)-(d) to achieve steady step response at low rated speed condition. Other than that, Figure 9 (a), (c) and (e) shows the simulated results are slower than experimental results in Figure 9 (b), (d) and (f) to achieve steady step response. Therefore, the PI controller is needed to improve for lower rated speed, but very outstanding at full rated and half rated speed commands with no load condition.

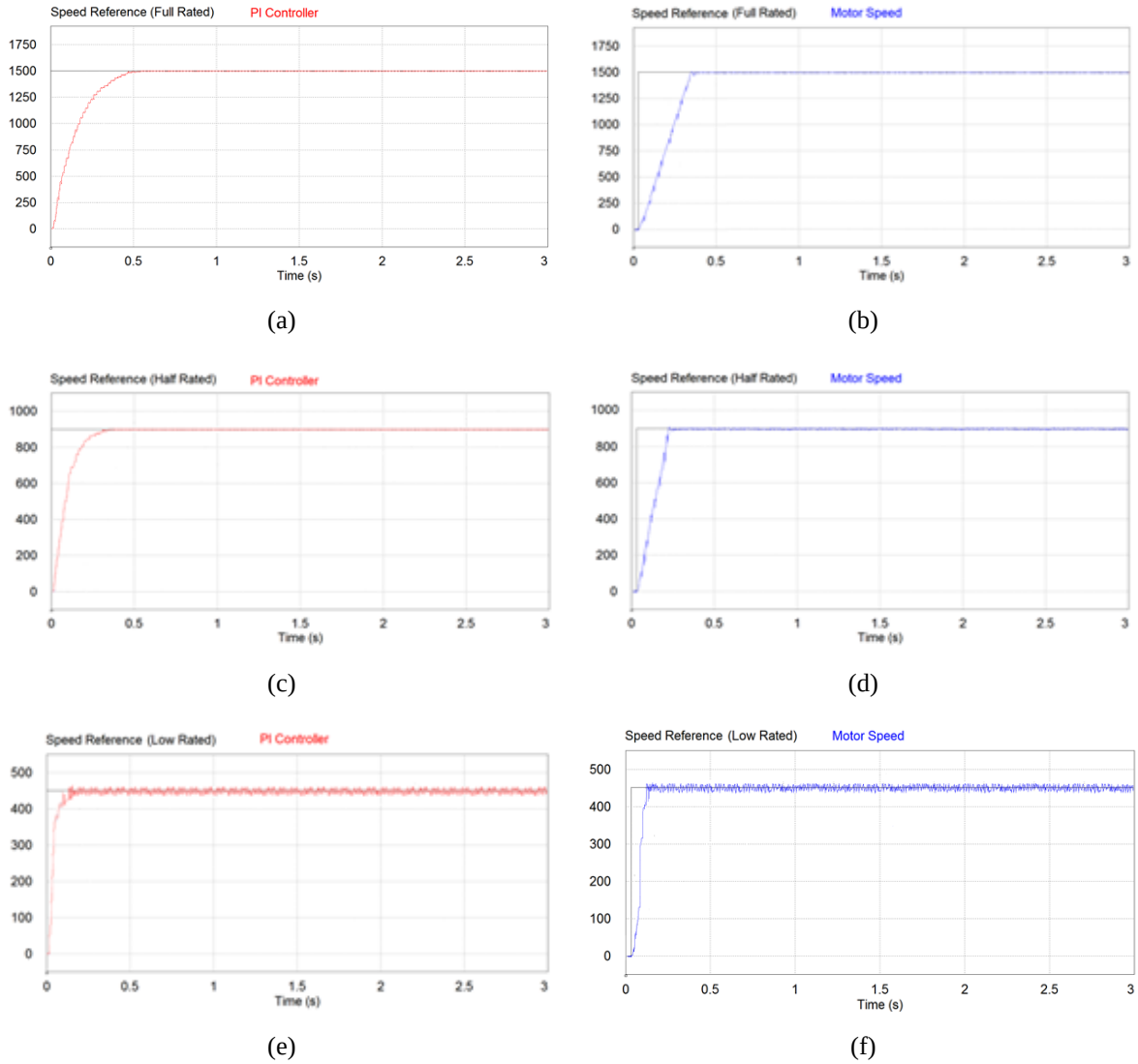

Figure 9. Simulated and experimental of PI results at; (a)-(b) full, (c)-(d) half and (e)-(f) low rated

6. CONCLUSION

In this paper, the performances of speed controller are demonstrated based on the sensored IFOC of three-phase induction motor. Basically, the simulated results are compared between P and PI controller at

differences speed commands with no load condition. The results are noted that the PI controller is more outstanding than the P controller in terms of performances which are faster to achieve steady state response, lower percentage of overshoot and oscillatory response. Besides, the simulated results of PI controller are compared with experimental results at differences speed commands with no load condition. In this regard, the comparing results are shows that the experimental results are faster than the simulated results in order to achieve steady state response. Moreover, PI controller is very outstanding at full rated and half rated speed commands with no load condition. However, the PI controller is needed to improve for lower rated speed condition. Finally, the results of simulated and experimental of IFOC for three-phase induction motor are valid indicator as a reference to improve control algorithm in future.

ACKNOWLEDGEMENTS

The authors would like to acknowledge Politeknik Merlimau Melaka (PMM) and Universiti Teknikal Malaysia Melaka (UTeM) through the grant FRGS/1/2015/TK04/JPP/03/1 Ministry of Higher Education Malaysia for their inspirations and supports.

REFERENCES

[1] F. A. Patakor, *et al.*, "Auto-tuning Sliding Mode Control for Induction Motor Drives," *2016 8th Comput. Sci. Electron. Eng. Conf.*, pp. 1–6, 2016.
[2] Z. Yongchang, *et al.*, "Comparative study of PI, sliding mode and fuzzy logic controller for rotor field oriented controlled induction motor drives," *Electr. Mach. Syst.*, vol. 1, no. 3, pp. 1089–1094, 2008.
[3] K. Wang, *et al.*, "An online rotor time constant estimator for the induction machine," *IEEE Trans. Control Syst. Technol.*, vol. 15, no. 2, pp. 339–348, 2007.
[4] S. R. Shaw, *et al.*, "Identification of induction motor parameters from transient stator current measurements," *IEEE Trans. Ind. Electron.*, vol. 46, no. 1, pp. 139–149, 1999.
[5] D. Telford, *et al.*, "Online identification of induction machine electrical parameters for vector control loop tuning," *IEEE Trans. Ind. Electron.*, vol. 50, no. 2, pp. 253–261, 2003.
[6] K. Bouhoune, *et al.*, "Hybrid control of the three phase induction machine using artificial neural networks and fuzzy logic," *Appl. Soft Comput.*, vol. 55, pp. 289–301, 2017.
[7] S. Masumpoor, *et al.*, "Adaptive sliding-mode type-2 neuro-fuzzy control of an induction motor," *Expert Syst. Appl.*, vol. 42, no. 19, pp. 6635–6647, 2015.
[8] C. L. Graciola, *et al.*, "Neural speed estimator for line-connected induction motor embedded in a digital processor," *Appl. Soft Comput. J.*, vol. 40, pp. 616–623, 2016.
[9] K. Zeb, *et al.*, "Indirect field-oriented control of induction motor drive based on adaptive fuzzy logic controller," *Electr. Eng.*, 2016.
[10] O. Ellabban, *et al.*, "Predictive torque control of an induction motor fed by a bidirectional quasi Z-source inverter," *IECON Proc. Industrial Electron. Conf.*, vol. 2, pp. 5854–5859, 2013.
[11] F. A. Patakor, *et al.*, "Adaptive Sliding Mode for indirect field oriented controlled of induction motor," *2011 IEEE Student Conf. Res. Dev.*, no. 4, pp. 289–293, 2011.
[12] J. A. Ali, *et al.*, "Improved Indirect Field-Oriented Control of Induction Motor Drive Based PSO Algorithm," *Jurnal Teknologi*, vol. 2, pp. 1–6, 2013.
[13] B. Akin and M. Bhardwaj, "Sensored Field Oriented Control of 3-Phase Permanent Magnet Synchronous Motors," *Texas Instruments, Inc. C2000 Systems and Applications*, 2013
[14] B. Popadic, *et al.*, "Tuning methods for PI controller - Comparison on a highly modular drive," *IYCE 2013 - 4th Int. Youth Conf. Energy*, 2013.
[15] M. Korkmaz, *et al.*, "Design and performance comparison of variable parameter nonlinear PID controller and genetic algorithm based PID controller," *INISTA 2012 - Int. Symp. Innov. Intell. Syst. Appl.*, 2012.
[16] B. W. Bequette, "Process Control: Modeling, Design, and Simulation," *Prentice Hall PTR*, 2003.

BIOGRAPHIES OF AUTHORS

Hasif Aziri was born in Kelantan, Malaysia, in 1991. He received his Diploma in Electronic Engineering from the Politeknik Kota Bharu (PKB), Kelantan, Malaysia, in 2013, and Bachelors Degree in Mechatronic Engineering with Honours from the Universiti Teknikal Malaysia Melaka (UTeM), Melaka, Malaysia, in 2016. He is currently working towards his Masters of Science in Electrical Engineering at the Universiti Teknikal Malaysia Melaka (UTeM), Melaka, Malaysia. He has been an Assistant Researcher at Universiti Teknikal Malaysia Melaka (UTeM) and Politeknik Merlimau Melaka (PMM) since 2016. His current research interests include fuzzy logic control, power electronics and motor drives.

Fizatul Aini Patakor was born in Selangor, Malaysia, in 1978. She received her Bachelors Degree in Electrical Engineering (Power Electrical) from the Universiti Sains Malaysia (USM), Penang, Malaysia, in 2001, the Master of Science in Occupational Safety and Health from the Universiti Utara Malaysia (UUM), Kedah, Malaysia, in 2008, and Doctor of Philosophy in Electrical Enginnering from the Universiti Teknikal Malaysia Melaka (UTeM), Melaka, Malaysia, in 2014. She is currently a Senior Lecturer at Politeknik Merlimau Melaka (PMM), Melaka, Malaysia and her interest includes safety and health in engineering education, power electronic and drives control system.

Marizan Sulaiman was born in Terengganu, Malaysia, in 1962. He received his Bachelor of Science in Electrical Engineering in May 1984, the Master of Science in Electrical Engineering in December 1985, and Doctor of Philosophy in Electrical Engineering in May 1989 from the University of Missouri, Columbia, U.S. He is a registered member of the Board of Engineers, Malaysia (BEM) and the Institution of Engineers, Malaysia (IEM). He is currently a Professor and has been appointed as the Director of Research and Innovation Management Center (CRIM) at Universiti Teknikal Malaysia Melaka (UTeM), Melaka, Malaysia. His research interests include electrical power system and control engineering.

Zulhisyam Salleh was born in Kedah, Malaysia, in 1977. He received his Bachelors Degree in Electrical and Electronic Engineering from the Universiti Sains Malaysia (USM), Penang, Malaysia, in 2001 and the Master of Science in Occupational Safety and Health from the Universiti Utara Malaysia (UUM), Kedah, Malaysia, in 2008. He is currently a Senior Lecturer at Politeknik Melaka (PMK), Melaka, Malaysia and working towards his Doctor of Philosophy in Electrical Enginnering at the Universiti Teknikal Malaysia Melaka (UTeM), Melaka, Malaysia. His current research interests include safety and health in engineering education, fuzzy logic control, power electronics and motor drives.